International Journal of Technology

Sustainable Porous Silica Material Extracted from Volcanic Ash of Mount Sinabung Indonesia as Corrosion Inhibitor

Lisnawaty Simatupang[1*], Rikson Siburian[2], Elfrida Ginting[1], Binsar Maruli Tua Pakpahan[3], Kristian Adinata Pratama Simatupang[1], Dea Gracella Siagian[1], Edward Relius Laoli[1], Ronn Goei[4], Alfred Iing Yoong Tok[4]

[1]*Department of Chemistry, Faculty of Mathematics and Natural Sciences, Universitas Negeri Medan, Jl. Willem Iskandar Psr. V, Medan Sumatera Utara, 20221, Indonesia*
[2]*Department of Chemistry, Faculty of Mathematics and Natural Sciences, Universitas Sumatera Utara, 20155, Medan, Indonesia*
[3]*Department of Mechanical Engineering, Faculty of Engineering, Universitas Negeri Medan, Jl. Willem Iskandar Psr. V, Medan Sumatera Utara, 2022, Indonesia*
[4]*School of Materials Science and Engineering, Nanyang Technological University, 50 Nanyang Avenue, 639798, Singapore*

Abstract. This study investigated the potential of porous silica material extracted from volcanic ash of Mount Sinabung, Indonesia, as a corrosion inhibitor. The new material was subjected to comprehensive analysis using the X-Ray Diffraction (XRD), Fourier Transform Infrared Spectroscopy (FTIR), Search Engine Marketing (SEM), and Atomic Absorption Spectrophotometry (AAS). Corrosion test was conducted by coating the metal surface with synthesized silica. XRD data showed the presence of amorphous silica, while SEM indicated a rough and irregular pore cavity. Based on AAS characterization, the concentration of silica in the Mount Sinabung volcanic ash was 79.23 % (v/v) with a yield of 29.73 %(w/w). Furthermore, coated and uncoated iron plates, with grit variations of 800, 1200, 1500, and 2000, were tested against HCl 15 % ($^v/_v$) and NaCl 3.5 % ($^w/_v$) as model corrosive solutions. The SEM results showed that coated plates had fewer holes and cracks formation while the XRD analysis of the same samples presented a slight decrease in the intensity of iron phase. Among silica-coated iron plates, the 1500 grit variation had the lowest corrosion rate and the highest corrosion inhibitor efficiency in both HCl 15 % ($^v/_v$) and NaCl 3.5 % ($^w/_v$) corrosive solutions, recording efficiencies of 26.3 and 91.8 %, respectively.

Keywords: Corrosion inhibitor; Grit; Natural silica; Silica coated iron; Volcanic ash

1. Introduction

Mount Sinabung is one of the active volcanoes in Indonesia, located in the North Sumatera Province. According to The Indonesia Disaster Control Bureau (BNPB) data, Mount Sinabung has emitted approximately 250 million tons of ash since the eruption in 2010. A previous study discovered that the main component of volcanic ash was SiO_2 (74.3%) (Karolina *et al.,* 2020; Lubis *et al.,* 2019). Silica content is higher compared to other volcanoes in the country, such as Mount Merapi (63.3 %) or Mount Kelud (70.6 %) (Nakada *et al.,* 2019).

The abundance of volcanic ash and high silica content presents significant potential for the production of silica-based material. Silica has various applications in the pharmaceutical, ceramics, paints, coatings, and chemical industries. This is due to the numerous advantageous properties, including high porosity, mechanical strength, thermal stability, pore surface area, stability in acidic environments, non-swelling characteristics, and resistance to microbial attack (Salleh *et al.,* 2021; Boonmee and Jarukumjorn, 2020; Pan, Li, and Mao., 2020; Mainier *et al.,* 2018a; El-Fargani *et al.,* 2017; Verma and Khan, 2016; Anderson and Segall, 2011). These attributes support the potential for the cost-effective production of silica-based composite material applied by various niche (Beleuk-a Moungam *et al.,* 2022; Prabha *et al.,* 2021; Silvana and Sunardi, 2020; Iguchi *et al.,* 2012).

Several studies have reported the use of volcanic ash, including its application as a base material for geopolymers and in the synthesis of nano-silica (Hasanah *et al.,* 2021; Sinuhaji *et al.,* 2018; Karolina *et al.,* 2015). Investigation has been conducted on the preparation of volcanic ash from Mount Sinabung, a basic material for creating silica-based adsorbents. This study also comprises the characterization of volcanic ash, modification of silica surfaces for composite material, and its application in heavy metal adsorption (Simatupang and Devi, 2016). Based on previous work, the characterization showed that the resulting silica gel was amorphous, with a surface area of 375 m^2/g and a pore diameter of 1.5 nm (Simatupang *et al.,* 2020). The substantial pore surface area renders silica gel suitable for adsorption purposes.

The common problem faced by industrialized nations is metal corrosion, a process driven by oxidation reactions, thereby leading to degradation in the quality of metal. Corrosion could be caused by moisture, acids, salt, and high ambient temperatures (Pan *et al.,* 2020; Yeganeh, Omidi, and Eskandari, 2018; Javaherdashti, 2000). However, the process can be controlled by slowing down oxidation (Assassi and Benharrats, 2021; Chasse, Scardino, and Swain, 2020; Wang *et al.,* 2020; Onyeachu *et al.,* 2019; Tansug *et al.,* 2014). The adhesion strength between the coating material and the ferrous metal surface is influenced by the level of surface roughness. The rough iron plate specimens produced areas with an unstable surface structure that experienced greater corrosion due to the uneven distribution of the passive layer.

Several materials previously used as corrosion inhibitor, include polyaniline, metal alloy, and imidiazole. Furthermore, inhibitor material characteristics are surface area, small pore size and heteroatom with N and O, lone pair electrons, as well as metal with lower potential reduction standard (Mulyani *et al.,* 2023; Ningrum *et al.,* 2023; Riyanto *et al.,* 2023; Assassi and Benharrats, 2021).

Sodium silicate is a chemical compound that is often used as corrosion inhibitor due to its environmentally friendliness and low cost (Mulyani *et al.,* 2023; Da-Silva, Saji, and Aoki, 2022; Saji, 2019). In coating application, a mixture of silica from natural sand and rice husk ash serves as a natural inhibitor for reinforcing concrete structures (Marzorati, Verotta, and Trasatti, 2019; Awizar *et al.,* 2013). This study was conducted specially to optimize the use of Sinabung volcanic ash as silica precursor and coating material for corrosion inhibitor to protect the ferrous metal from corrosion.

2. Methods

2.1. Preparation of Silicate from Volcanic ash

The preparation of silicate comprised soaking 20 g of volcanic ash in 37 % ($^v/_v$) HCl (E-Merck) for 2 hours at a temperature of 95°C with continuous stirring. After filtration,

the residue was rinsed in distilled water until reaching pH 7, then dried in an oven at 120 °C for 6 hours. The dried volcanic ash was extracted with a 4, 6, or 8 M NaOH solution (E-Merck) and boiled while stirring until the mixture thickened. The mixture was then placed in a furnace at 750 °C for 3 hours. After cooling, 200 mL of distilled water was added, and the mixture was left overnight before being filtered. A total of 20 mL of Na_2SiO_3 solution was placed into a plastic container, and a few drops of 3M HCl solution were added while stirring to form a white gel and neutral pH. Silica gel was filtered and rinsed with distilled water, followed by drying in an oven at 120 °C. Silica yield from volcanic ash was calculated using Equation 1.

$$\% \text{ silica} = \frac{initial\ mass\ ash}{final\ mass\ ash} \times 100\% \tag{1}$$

The schematic representation of the preparation of silica from volcanic ash is shown in Figure 1.
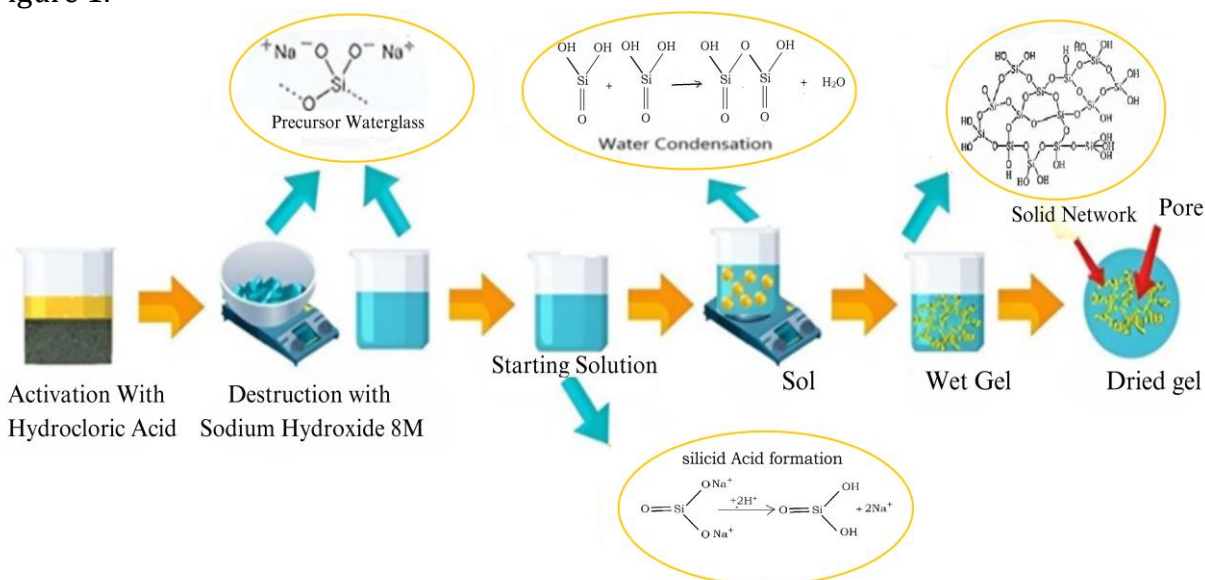
Figure 1 A Schematic Representation of the Preparation of Silica from Volcanic Ash

Atomic Absorption Spectroscopy (AAS)Z-2000 series was performed to determine silica content in the Na_2SiO_3 solution. FTIR SHIMADZU, Rigaku ZSX, XRD Perkin Elmer 3110 Shimadzu XRD 6000, and SEM Zeiss type EPOMH 10 Zss were used to characterize the physicochemical properties of material.

2.2. Corrosion Testing of Iron Samples

Iron plate 3 × 3 cm^2 with a thickness of 3 mm was used for corrosion testing. The samples were pre-treated with sandpaper of varying grit numbers 800, 1200, 1500, and 2000 to smoothen and remove scratches on the surface. Each iron plate grit was soaked in Inhibitor for 5 days. Subsequently, the uncoated and coated iron plates were dipped in a corrosive solution containing 15 % ($^v/_v$) HCl and 3.5 % ($^w/_v$) NaCl for 96 hours. The HCl solution represents an acidic environment while NaCl represents a salty atmosphere conducive to corrosion. Sets of silica-coated and uncoated iron plates were analyzed using SEM and XRD before and after corrosion tests.

3. Results and Discussion

Peaks at 3356.89 cm^{-1}, 3454.12 cm^{-1}, and 3446.02 cm^{-1}, showed the presence of OH strain vibrations from Si-OH, as presented in Figure 2. Furthermore, Si-O asymmetric stretching vibrations in Si-O-Si were characterized by band absorptions at 1184.45 cm^{-1}

and 1095.57 cm^{-1}, represented by a wide and sharp peak in the 1000-1100 cm^{-1} wavenumber range. A peak was observed at wave numbers 796.42 cm^{-1} and 789.21 cm^{-1}, which showed Si-O-Si stretching vibrations. The presence of the Si-O-Si functional group was confirmed by the peaks observed at 326.46 cm^{-1}, attributed to the bending vibration, in both 6M and 8M NaOH solutions.

The XRD pattern, as presented in Figure 2, showed that silica gel produced from the 3 variations of NaOH was amorphous, characterized by a broad peak at 2θ = 23.36°; 2θ = 22.68°; 2θ = 23.40°, with the highest intensity being 2θ = 23.40°. The diffraction pattern, with a peak, widened around 2θ = 20-24°, indicated a low crystallinity amorphous structure (Simatupang *et al.,* 2018).

SEM image showed the existence of rough and irregular pore cavities, as presented in Figure 3. The presence of amorphous silica was also confirmed by the XRD results. Non-crystalline or amorphous silica possesses pores with atoms or molecules arranged in random and irregular patterns, as well as complex spherical structures.

(1)   (2)
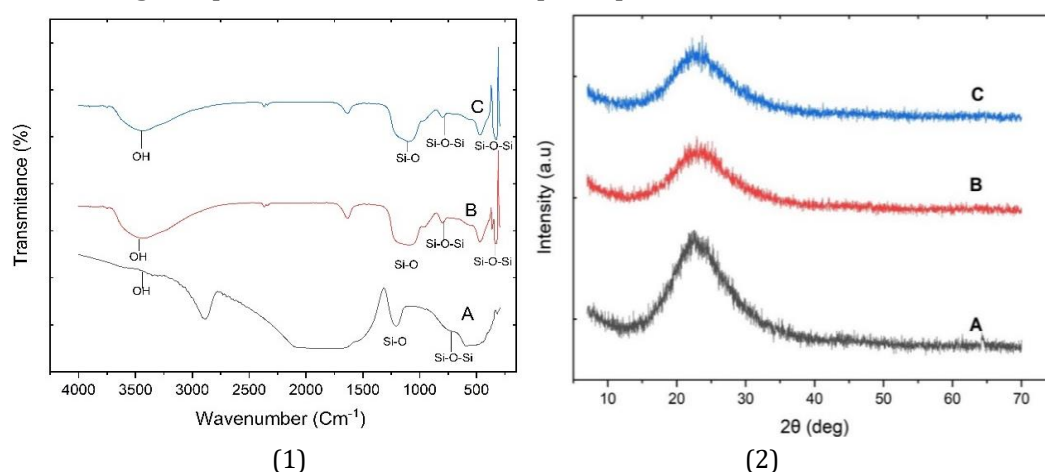
Figure 2 (1) FTIR spectra of silica gel prepared using (A) 4M NaOH, (B) 6M NaOH, and (C) 8M NaOH, and (2) XRD pattern spectra of silica gel prepared using (A) 4M NaOH, (B) 6M NaOH, and (C) 8M NaOH
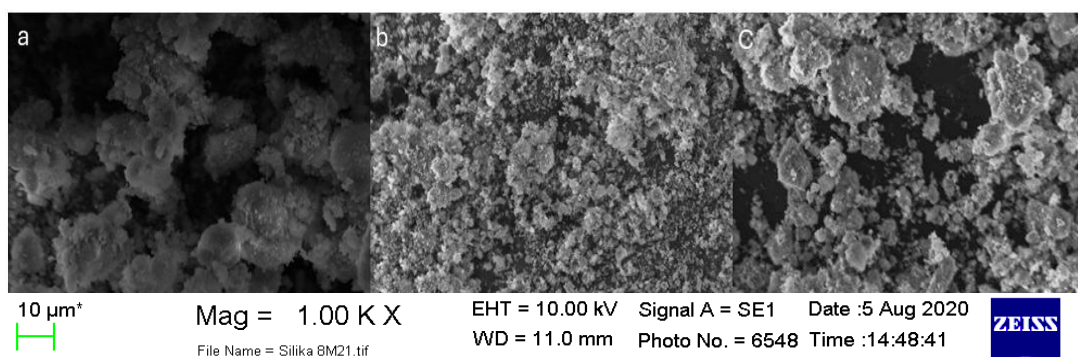

Figure 3 SEM Image of Silica Gel Prepared Using (a) 4M NaOH, (b) 6M NaOH, (c) 8M NaOH

The concentration of NaOH and the length of the extraction time affect silica formation process. The AAS data showed that the highest silica content was discovered when volcanic ash was extracted with 8M NaOH solution. This concentration resulted in a 79.23% (v/v) Na_2SiO_3 and a gel yield of 29.73% (w/w). The purpose of using 8M NaOH is due to the higher concentration of NaOH, leading to greater extraction power.

The sets of silicate-coated and uncoated iron plates were subjected to corrosion test using a corrosive solution containing 15 % HCl ($^v/_v$) and 3.5 % NaCl ($^w/_v$). The results were analyzed using SEM (Figures 4 and 5).

The morphology of an uncoated 800-grit iron plate soaked in 15 % HCl ($^v/_v$) showed many holes in the pores due to corrosion. The surface of iron plate was also uneven, and many cracks were observed. Similar trends were observed for iron plates with 1200 and 2000 grit, which had lumps and relatively large holes on the surface due to corrosion. The surface of the 1500 grit iron plate was smoother compared to the 800, 1200, and 800 grit. When a 1500-grit iron plate without a coating is soaked in 15 % HCl ($^v/_v$), a few small holes were observed in the surface pores.
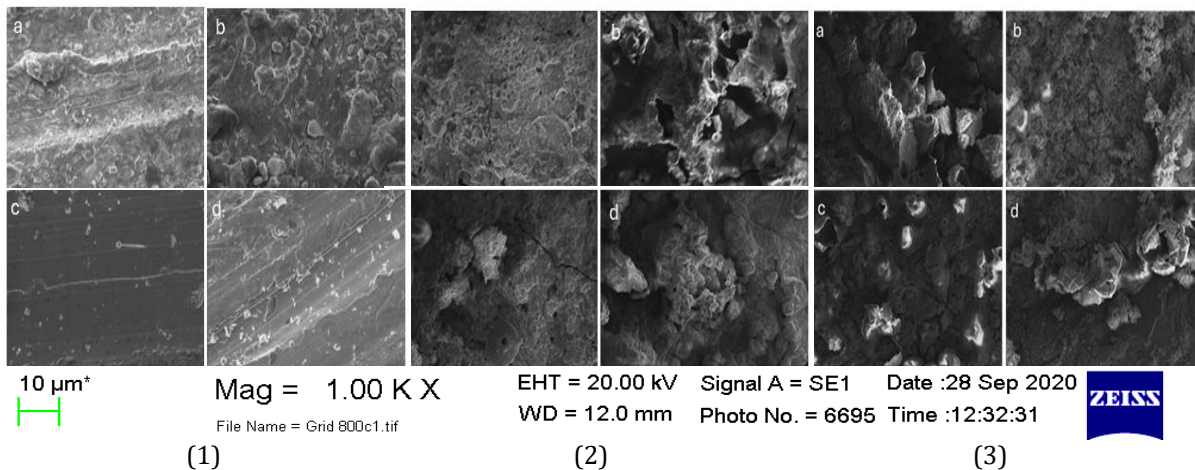
Figure 4 (1) SEM images grit of iron plate uncoated before treatment (a) 800 (b) 1200 (c) 1500 (d) 2000; (2) SEM images uncoated, in HCl 15 % ($^v/_v$); (3) SEM images uncoated, in NaCl 3.5 % ($^w/_v$)

The corrosive solution of 3.5 % NaCl used for each grit of the uncoated iron plate, caused the holes, lumps, and cracks on the surface due to deposits from the reaction of Fe with a salt electrolyte solution. The reaction time is directly proportional to the precipitate produced. Pitching corrosion can be observed in cases where chloride ions accumulate locally on the rougher surface in amounts greater than the threshold value (Riyanto *et al.,* 2023).
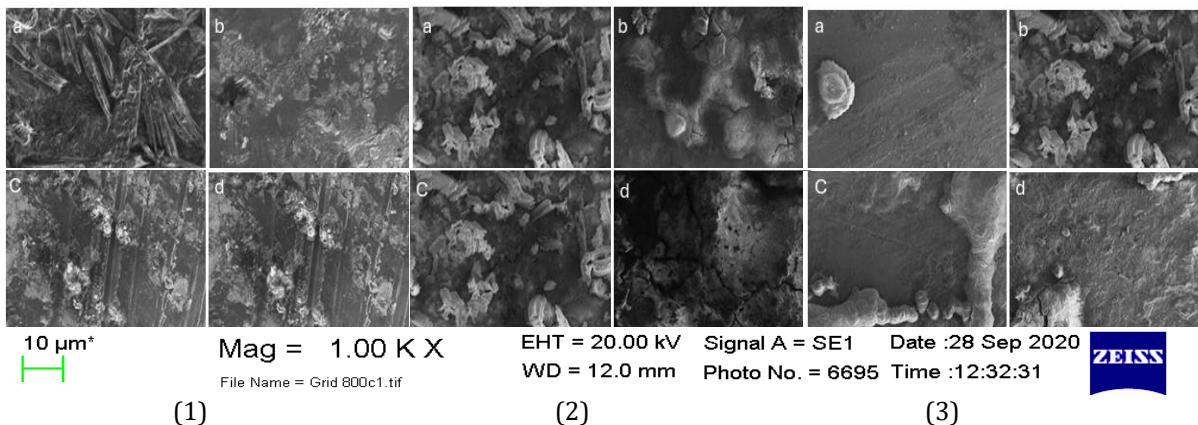
Figure 5 (1) SEM images of grit of iron plate coated before treatment, showing (a) 800, (b) 1200, (c) 1500, and (d) 2000 grit levels; (2) SEM images of coated iron plate after exposure to 15 % HCl ($^v/_v$); and (3) SEM images of coated iron plate after exposure to 3.5 % NaCl ($^w/_v$)"

Figure 5 shows the morphology of iron plate after coating with silicate. The 1500-grit iron plate has the smoothest surface compared to the other grits, which results in a more even thickness of silicate layer. The morphology appeared to be less perforated and fewer lumps were formed compared to uncoated iron plates with inhibitor. This is in accordance with the theory that samples with the addition of inhibitor will crack less, showing a smaller corrosion rate (Devianto *et al.,* 2023; Goyal *et al.,* 2020). Based on the analysis data, it was observed that silicate is effective as corrosion inhibitor.

The reaction mechanism scheme is shown in Figure 6. Sodium silicate has an anodic inhibitory capacity in a neutral medium. This implied that the SiO_2 species migrated to the anode region of the metal surface, reacting with Fe^{2+} ions and forming a protective layer of iron silicate ($FeSiO_3$). Silicate was effective as inhibitor by reacting with OH-, thereby reducing corrosion reaction in neutral solutions and decreasing corrosion rate. The new peak that appeared after immersion at $2\theta = 30\text{-}40°$ was $FeOOH^-$ (Ningrum *et al.,* 2023).
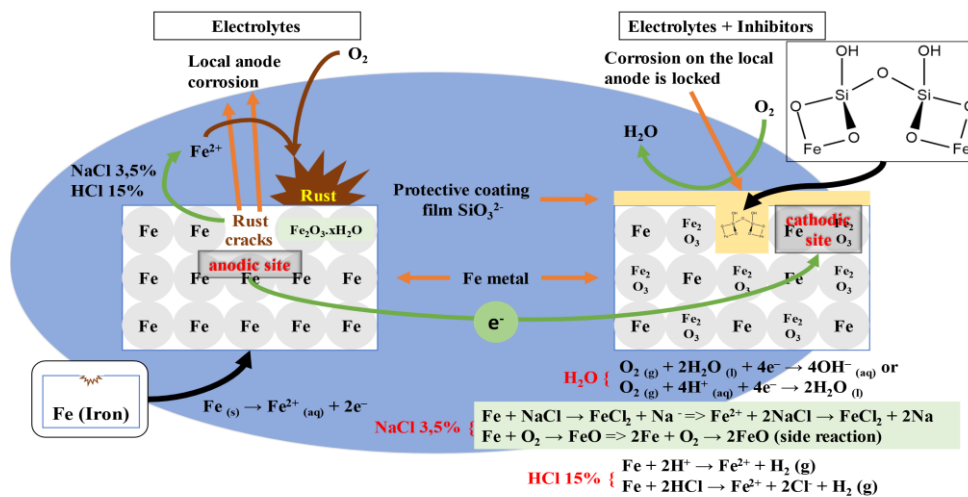
Figure 6 Mechanism of silicate inhibition reaction

XRD patterns for all grit both uncoated and coated iron plates in NaCl 3.5% (w/v) can be seen in Figure 7 showing that the peak on iron plate was lower in intensity than the peak on iron plate before treatment.
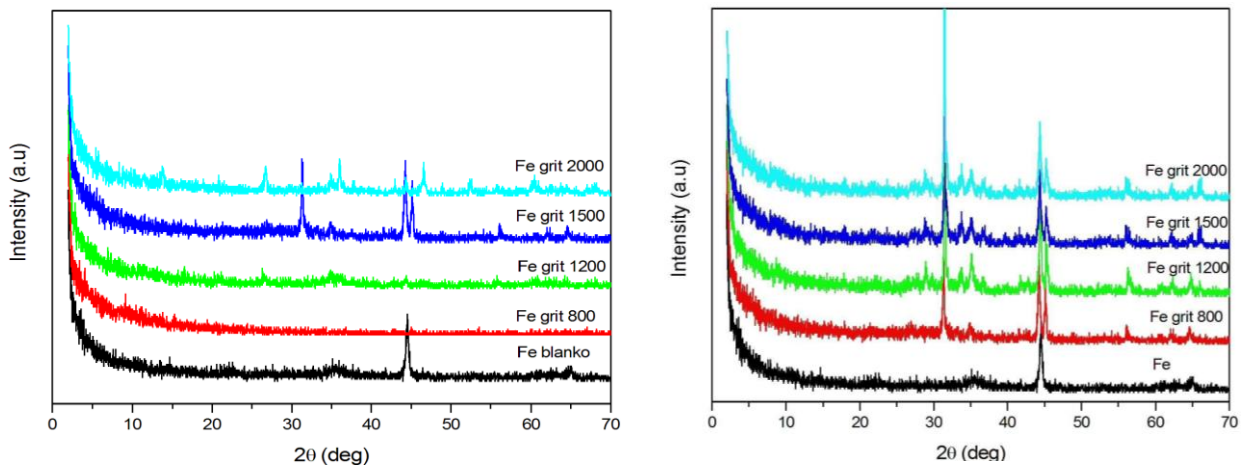
Figure 7 XRD patterns diffractogram of uncoated iron plate and coated iron plate immersed in NaCl 3.5 % ($^w/_v$)

The existence of a lower intensity peak after immersion in corrosion solution showed sediment. The Fe peak of the 2000 grit iron plate at $2\theta = 40\text{-}50°$ was sharper compared to

the 1200 and 1500 grit. Furthermore, the level of surface smoothness affected corrosion rate, with a new peak appearing at $2\theta = 20$-$30°$ for the series of samples after immersion in NaCl 3.5% (w/v). The intensity of each iron plate showed a reduction in iron corrosion rate and a slight decrease in grit size variation, showing effective inhibition by silicate inhibitor.

Corrosion test of iron plate was analyzed for corrosion rate using the weight-loss method (Malaret, 2022). Where the CR is corrosion rate (mpy), W is mass loss (g), A is surface area (cm^2), t is the exposure time (hour), D is density (g/cm^3), C is constant 3.45 x 10^6.
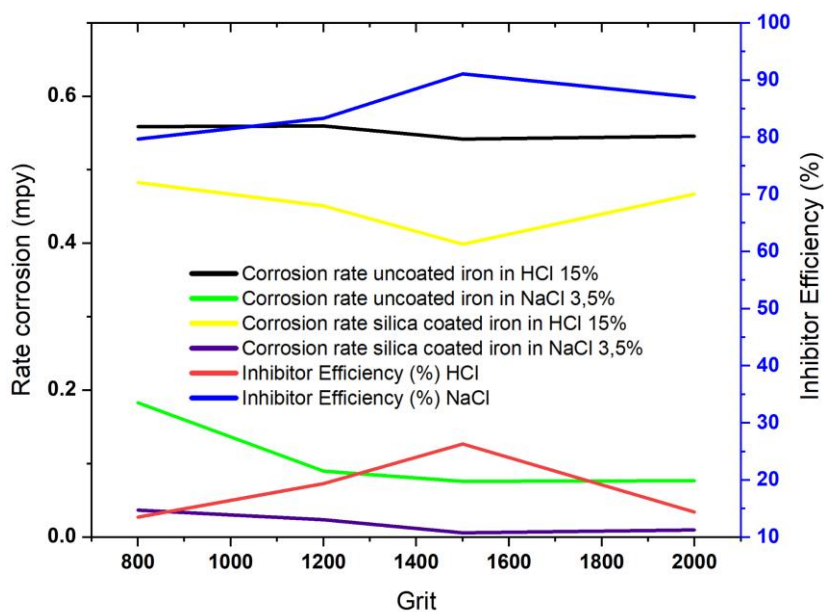
$$CR = \frac{C.W}{D.A.t} \tag{2}$$

$$\text{inhibitor efficiency} = \frac{CR\ non\ additives - CR\ additives}{CR\ non\ Additives} \tag{3}$$

Based on Table 1, the 1500 grit iron plate, whether silica-coated or uncoated, had lowest corrosion rate of 3.399 mpy and 0.006 mpy, alongside highest inhibitor efficiency of 26.3% and 91.1% respectively. These results surpass those of a previous study utilizing tobacco extract and sodium silicate as inhibitor in a3.5% NaCl (w/v) corrosive solution, which achieved efficiencies of 24 - 69% and 79.55%, respectively.

Table 1 Data of Corrosion Rate and Inhibitor Efficiency for each Grit of Iron Plate

No	Grit	Corrosion Solution	Corrosion rate uncoated iron (mpy)	Corrosion rate silicate-coated iron (mpy)	Inhibitor Efficiency (%)
1	800		0.559	0.483	13.5
2	1200	HCl 15%	0.560	0.451	19.4
3	1500		0.542	0.399	26.3
4	2000		0.546	0.467	14.4
5	800		0.183	0.037	79.7
6	1200	NaCl 3.5%	0.090	0.024	83.3
7	1500		0.076	0.006	91.1
8	2000		0.077	0.010	87.0

Figure 8 Corrosion Rate and Inhibitor Efficiency for each Grit of Iron Plate uncoated silica inhibitor and coated silica inhibitor in corrosive solutions

4. Conclusions

In conclusion, the highest silica content from volcanic ash of Mount Sinabung was observed when 8M NaOH was used, with a Na_2SiO_3 concentration of 79.23 v% ($^v/_v$) and a yield of 29.73v% ($^w/_w$). According to the characterization results by FTIR, the synthesized silica gel has -OH and Si-O functional groups from Si-OH and Si-O-Si, respectively. XRD analysis suggested that the as-synthesized silica gel had an amorphous structure. Micrograph SEM showed rough and irregular pore cavities, while the effect of surface grit variations on the performance of sodium silicate inhibitor synthesized in 15 % HCl ($^v/_v$) and 3.5 % NaCl ($^w/_v$) solutions, was lower corrosion rates. The lowest corrosion rate was observed on the 1500 grit iron plate, and the addition of silica as inhibitor reduced the rate in HCl 15 % ($^v/_v$) and NaCl 3.5 % ($^w/_v$) corrosive solutions, leading to inhibitor efficiencies of 26.3 % and 91.8 %, respectively.

Acknowledgments

References

Anderson, K., Segall, P., 2011. Physics-based Models of Ground Deformation and Extrusion Rate at Effusively Erupting Volcanoes. *Journal of Geophysical Research: Solid Earth,* Volume 16(B7), pp. 1–20

Assassi, F., Benharrats, N., 2021. Synthesis, Characterizations and Application of Polyaniline-paint as Anticorrosion Agent. *Inorganic and Nano-Metal Chemistry*, Volume 51(6), pp. 805–813

Awizar, D.A., Othman, N.K., Jalar, A., Daud, A.R., Rahman, I.A., Al-Hardan, N.H., 2013. Nanosilicate Extraction from Rice Husk ash as Green Corrosion Inhibitor. *International Journal of Electrochemical Science*, 8(2), 1759–1769

Beleuk-a Moungam, L.M., Lemougna, P.N., Kaze, R.C., Mohamed, H., Deutou-Nemaleu, J.G., Billong, N., Kamseu, E., Mvondo-Ze, A.D., Kenfack, I.T., 2022. Synthesis of Volcanic Ash-based Porous Inorganic Polymers Using Biomass as Pore Inducing Agent: Phase Evolution and Descriptive Microstructure. *Silicon*, Volume 14(6), pp. 2595–2608

Boonmee, A., Jarukumjorn, K., 2020. Preparation and Characterization of Silica Nanoparticles from Sugarcane Bagasse Ash for using as a Filler in Natural Rubber Composites. *Polymer Bulletin*, Volume 77(7), pp. 3457–3472

Chasse, K.R., Scardino, A.J., Swain, G.W., 2020. Corrosion and Fouling Study of Copper-based Antifouling Coatings on 5083 Aluminum Alloy. *Progress in Organic Coatings*, Volume 141, p. 105555

Da-Silva, P.B., Saji, V.S., Aoki, I.V., 2022. Rapid and Eco-friendly One-step Synthesis of Dodecylamine-encapsulated Mesoporous Silica Nanocontainers. *Microporous and Mesoporous Materials*, Volume 341, pp. 112109

Devianto, H., Nurdin, I., Widiatmoko, P., Silvia, D., Prakarsa, C., 2023. Tobacco Extract for Inhibition of Carbon Steel Corrosion in H2S-contained NaCl Solution. *International Journal of Technology,* Volume 14(5), pp. 1167–1176

El-Fargani, H., Lakhmiri, R., El-Farissi, H., Albourine, A., Safi, M., Cherkaoui, O., 2017. Removal of Anionic Dyes by Silica-chitosan Composite in Single and Binary Systems: Valorization of Shrimp co-product "Crangon-Crangon" and "Pandalus Borealis." *Journal of Materials and Environmental Science,* Volume 8(2), pp. 724–739

Goyal, M., Vashist, H., Kumar, S., Bahadur, I., Benhiba, F., Zarrouk, A., 2020. Acid Corrosion Inhibition of Ferrous and Non-ferrous Metal by Nature Friendly Ethoxycarbonylmethyltriphenylphosphonium Bromide (ECMTPB): Experimental and MD Simulation Evaluation. *Journal of Molecular Liquids*, Volume 315, p. 113705

Hasanah, M., Sembiring, T., Sebayang, K., Humaidi, S., Rahmadsyah, Saktisahdan, T.J., Handoko, F., Ritonga, S.I., 2021. Extraction Of Silica Dioxide (SiO_2) From Mount Sinabung Volcanic Ash with Coprecipitation Method. *In:* IOP Conference Series: Materials Science and Engineering, Volume 1156(1), p. 012015

Iguchi, M., Surono, Nishimura, T., Hendrasto, M., Rosadi, U., Ohkura, T., Triastuty, H., Basuki, A., Loeqman, A., Maryanto, S., Ishihara, K., Yoshimoto, M., Nakada, S., Hokanishi, N., 2012. Methods for Eruption Prediction and Hazard Evaluation at Indonesian Volcanoes. *Journal of Disaster Research*, Volume 7(1), pp. 26–36

Javaherdashti, R., 2000. How Corrosion Affects Industry and Life. *Anti-Corrosion Methods and Materials*, Volume 47(1), pp. 30–34

Karolina, R., Syahrizal, S., Putra, M.A., Prasetyo, T.A., 2015. Optimization of the use of Volcanic Ash of Mount Sinabung Eruption as the Substitution for Fine Aggregate. *Procedia Engineering*, Volume 125, pp. 669–674

Karolina, R., Syahrizal., M.A.P., Handana., Wijaya, B., 2020. Utilization of Volcanic Ash of Mount Sinabung as a Substitute for Cement to Flexure Strength of Geopolymer Concrete. *Icosteerr 2018*, pp. 332–337

Lubis, M., Sukeksi, L., Harahap, M.B., Ginting, M., Wici, H., Ayu, G.E., 2019. Use of Silica Gel from Volcanic Ash as Chitosan Composite Membrane's Filler. *Asian Journal of Chemistry*, Volume 31(10), pp. 2303–2305

Mainier, F.B., Figueiredo, A.A.M., de-Almeida Junior, A.A.M., Almeida-Junior, B.B., 2018a. Proposal of the use Sodium Silicate as a Corrosion Inhibitor in Hydrostatic Testing of Petroleum Tanks using Seawater. *International Journal of Advanced Engineering Research and Science*, Volume 5(6), pp. 33–38

Malaret, F., Yang, X.S., 2022. Exact Calculation of Corrosion Rates by the Weight-loss Method. *Experimental Results*, Volume 3, p. E13

Marzorati, S., Verotta, L., Trasatti, S.P., 2019. Green Corrosion Inhibitors from Natural Sources and Biomass Wastes. *Molecules*, Volume 24(1), p. 48

Mulyani, R.W.E., Nuruddin, A., Suprijanto, Sunendar-Purwasasmita, B., 2023. Silica-Chitosan Nanocomposite Coatings for Enhancing Hydrophilicity of Polyester Fabric. *International Journal of Technology*, Volume 14(4), pp. 761–769

Nakada, S., Zaennudin, A., Yoshimoto, M., Maeno, F., Suzuki, Y., Hokanishi, N., Sasaki, H., Iguchi, M., Ohkura, T., Gunawan, H., Triastuty, H., 2019. Growth process of the lava dome/flow complex at Sinabung Volcano during 2013–2016. *Journal of Volcanology and Geothermal Research*, Volume 382, 120–136

Ningrum, E.O., Khoiroh, I., Nastiti, H.I., Affan, R.A., Karisma, A.D., Agustiani, E., Surono, A., Suroto, H., Suprapto, S., Taji, L.S., Widiyanto, S., 2023. Surface Coating Effect on Corrosion Resistance of Titanium Alloy Bone Implants by Anodizing Method. *International Journal of Technology*, Volume 14(4), pp. 749–760

Onyeachu, I.B., Obot, I.B., Sorour, A.A., Abdul-Rashid, M.I., 2019. Green Corrosion Inhibitor for Oilfield Application I: Electrochemical Assessment of 2-(2-pyridyl) Benzimidazole for API X60 Steel Under Sweet Environment in NACE Brine ID196. *Corrosion Science*, Volume 150, pp. 183–193

Pan, C., Chen, N., He, J., Liu, S., Chen, K., Wang, P., Xu, P., 2020. Effects of Corrosion Inhibitor and Functional Components on the Electrochemical and Mechanical Properties of

Concrete Subject to Chloride Environment. *Construction and Building Materials*, Volume 260, p. 119724

Pan, C., Li, X., Mao, J., 2020. The Effect of a Corrosion Inhibitor on the Rehabilitation of Reinforced Concrete Containing Sea Sand and Seawater. *Materials*, Volume 13(6), p. 1480

Prabha, S., Durgalakshmi, D., Rajendran, S., Lichtfouse, E., 2021. Plant-derived Silica Nanoparticles and Composites for Biosensors, Bioimaging, Drug Delivery and Supercapacitors: a Review. *Environmental Chemistry Letters*, Volume 19(2), pp. 1667–1691

Riyanto, Jazuli, M.M., Sahroni, I., Musawwa, M.M., Cahyandaru, N., Wahyuni, E.T., 2023. A Simple Technique for the Corrosion Inhibition of Underwater Cannonball from a Shipwreck. *International Journal of Technology*, Volume14(4), pp. 843–853

Saji, V.S., 2019. Supramolecular Concepts and Approaches in Corrosion and Biofouling Prevention. *Corrosion Reviews*, Volume 37(3), pp. 187–230

Salleh, S.Z., Yusoff, A.H., Zakaria, S.K., Taib, M.A.A., Seman, A.A., Masri, M.N., Mohamad, M., Mamat, S., Sobri, S.A., Ali, A., Ter-Teo, P., 2021. Plant Extracts as Green Corrosion Inhibitor for Ferrous Metal Alloys: A Review. *Journal of Cleaner Production*, Volume 304, p. 127030

Silvana, S., Sunardi, S., 2020. Synthesis and Characterization of Si02/Zn0 Nanocomposites from Zinc Waste and Mount Merapi Volcanic Ash. *Journal of Scientific and Applied Chemistry*, Volume 23(10), pp. 365–369

Simatupang, L., Devi., 2016. The preparation and characterization of Sinabung volcanic ash as silica based adsorbent. *Jurnal Pendidikan Kimia (Journal of Chemistry Education)*, Volume 8(3), pp. 159–163

Simatupang, L., Siburian, R., Sitanggang, P., Doloksaribu, M., Situmorang, M., Marpaung, H., 2018. Synthesis and Application of Silica Gel Base on Mount Sinabung's Fly Ash for Cd(II) Removal with Fixed Bed Column. *Rasayan Journal of Chemistry*, Volume 11(2), p. 819–827

Simatupang, L., Situmorang, M., Marpaung, H., Siburian, R., 2020. Fabrication of Silica-based Chitosan Biocomposite Material from Volcanic Ash and Shrimp Husk by Sol Gel Method for Adsorbent of Cadmium (Ii) Ions. *Indian Journal of Chemical Technology*, Volume 27(5), pp. 387–394

Sinuhaji, P., Sembiring, T., Magfirah, A., Piliang, AF., Nababan, S.M., 2018. Analysis of Composition; Topography of Volcanic Materials Erupted from Mount Sinabung, Karo Regency, Indonesia. *In:* Journal of Physics: Conference Series, Volume 1116(3), p. 032035

Tansug, G., Tüken, T., Giray, E.S., Findikkiran, G., Siğircik, G., Demirkol, O., Erbil, M., 2014. A New Corrosion Inhibitor for Copper Protection. *Corrosion Science*, Volume 84, pp. 21–29

Verma, D.K., Khan, F., 2016. Corrosion Inhibition of Mild Steel in Hydrochloric Acid using Extract of Glycine Max Leaves. *Research on Chemical Intermediates*, Volume 42(4), pp. 3489–3506

Wang, X., Jing, C., Chen, Y., Wang, X., Zhao, G., Zhang, X., Wu, L., Liu, X., Dong, B., Zhang, Y., 2020. Active Corrosion Protection of Super-hydrophobic Corrosion Inhibitor Intercalated Mg–Al Layered Double Hydroxide Coating on AZ31 Magnesium Alloy. *Journal of Magnesium and Alloys,* Volume 8(1), pp. 291–300

Yeganeh, M., Omidi, M., Eskandari, M., 2018. Superhydrophobic Surface of AZ31 Alloy Fabricated by Chemical Treatment in the $NiSO_4$ Solution. *Journal of Materials Engineering and Performance*, Volume 27(8), pp. 3951–3960